A02-13562

AIAA 2002-0161
Optimal Vortex Ring Formation at the Exit of a Shock Tube

Kamran Mohseni
Department of Aerospace Engineering Sciences
University of Colorado, Boulder
CO 80309-0429

40th AIAA Aerospace Sciences Meeting and Exhibit
14-17 January 2002 / Reno, NV

AIAA 2002-0161

OPTIMAL VORTEX RING FORMATION AT THE EXIT OF A SHOCK TUBE

Kamran Mohseni

Department of Aerospace Engineering Sciences,
University of Colorado at Boulder, CO 80309-0429,
mohseni@colorado.edu

Abstract

Formation of vortex rings at the exit of a shock tube is studied theoretically. A model for predicting the maximum circulation that a vortex ring can attain at the exit of a shock tube is offered. To achieve maximum circulation the initial conditions and the design of the driver and driven sections must be such that the generated shock wave reaches the shock tube exit at least $4D_n/u_2$ time units (D_n is the nozzle diameter and u_2 is the fluid velocity behind the shock wave) before the leading front of the expansion waves arrives at the shock tube exit. A simple way to satisfy this condition is to design a shock tube with long driver and short driven sections. The model is verified by comparison with available computational and experimental data.

1 Introduction

The first shock tube was invented by Vieille[1] in 1899 for investigation on the flame propagation problem. Shock tubes are now a common tools for the study of gas dynamic problems. A shock tube converts the potential energy stored in the pressurized gas to accelerate the fluid inside the shock tube. There are many variety of shock tubes available now. While the design and the range of applicability of various shock tubes are different their working principles are very similar. In this study we will focus on a simple but widely used shock tube, that is a constant-area shock tube with a diaphragm separating the low- and high-pressure regions. Our analysis can be easily extended to other designs of shock tubes as discussed in §6.

Vortex rings are one of the simplest three dimensional coherent structures in fluid flows. They are very persistent structures and decay only very slowly at high Reynolds number. The formation and propagation of vortex rings attracted many researchers over the last century. von Karman & Burgers[2] studied vortex ring generation by an impulsive pressure acting over a circular area. Another method of generating vortex rings is by impulsive acceleration of the air at the open end of a shock tube by the emergence of the generated shock wave when the shock tube is fired. The formation of a vortex ring at the exit of a tube by an emerging shock wave was established by Gawthrop, Shepherd and Perrott[3] in 1931. They generated the shock wave by detonation of an explosive charge at the opposite end of the tube. Elaborate photographs of such vortex rings was provided by Sturtevant.[4] Usually the resulting vortex rings are turbulent and very energetic. The advantage of this method of vortex ring generation is that the flow field in the tube is almost perfectly uniform and well-defined.

Different initial conditions and designs of the driver and driven sections of a shock tube result in the formation of vortex rings with various size, circulation, propagation speed, *etc.* In this paper conditions for generating an optimal vortex ring, with maximal circulation, at the exit of a shock tube is investigated. Such vortex rings have also maximal mixing properties.[8]

Vortex ring formation at the exit of a tube is a complicated process even in the incompressible case and no comprehensive theoretical description is available. The compressible Hill's spherical vortex was recently studied by Moore & Pullin.[5] The initial stage of the vortex ring formation in the incompressible flows (applicable only to thin core vortex rings) is described by the local similarity theory of the flow near a sharp edge offered by Pullin,[6] which was generally confirmed in the water tank experimental study of Didden.[7]

This paper is organized as follows. In the next section we review the relaxational approach in the vortex ring pinch-off process. This will motivate the application of the same approach to the vortex ring pinch-off process at the exit of a shock tube. Theory of shock tubes will be reviewed in section 3. A vortex

ring pinch-off model is developed in section 4 and a computational procedure for its implementation will be discussed in section 5. In section 6 our vortex ring pinch-off criteria is compared with some available experimental and computational data. Finally we summarize our results in section 7.

2 Universality in vortex ring pinch-off process

Generation, formation, evolution, and interactions of vortex rings have been the subject of numerous studies (*e.g.*, Shariff & Leonard[9] and the references therein). However, we focus our attention on a specific characteristic of vortex ring formation; namely the vortex ring pinch-off process.[10] In a laboratory, incompressible vortex rings can be generated by the motion of a piston pushing a column of fluid through an orifice or nozzle. The boundary layer at the edge of the orifice or nozzle will separate and roll up into a vortex ring. Gharib *et al.*[10] observed that for large piston stroke versus diameter ratios (L/D), the generated flow field consists of a leading vortex ring followed by a trailing jet.[10] The vorticity field of the formed leading vortex ring is disconnected from that of the trailing jet at a critical value of L/D (dubbed the "formation number"), at which time the vortex ring attains a maximum circulation. The formation number was in the range 3.6 to 4.5 for a variety of exit diameters, exit plane geometries, and non-impulsive piston velocities. Mohseni & Gharib[11] offered a relaxational model for the vortex ring pinch-off process. Numerical simulations of the Navier-Stokes equations were performed by Mohseni *et al.*[12] where they verified the modeling assumptions in Mohseni & Gharib.[11] An explanation for this phenomenon was given based on Kelvin's variational principle. It was both experimentally[10] and analytically[11] observed that the limiting stroke L/D occurs when the generating apparatus is no longer able to deliver energy E, circulation Γ and impulse I at a rate comparable with the requirement that a steadily translating vortex ring has maximum energy with respect to kinematically allowable perturbations.

Recently Mohseni[13] argued that the energy extremization in Kelvin's variational principle has a close connection with the entropy maximization in statistical equilibrium theories. We think that since the formation of vortex rings involves strong mixing of the generated shear layer with the ambient fluid (the same applies to the formation of vortices in two-dimensional flows), the ergodicity requirement of statistical equilibrium theories has a chance to be satisfied. Inspired by these observations we offered a relaxational (statistical) approach to the vortex ring pinch-off process.[11,13] Numerical evidence for a relaxation process in axisymmetric flows to an equilibrium state has already been provided in a direct numerical simulation of the vortex ring pinch-off process.[12] Mixing entropy miximization offers an alternative explanation of the vortex ring pinch-off process besides the energy extremization approach in Kelvin's variational principle. From this point of view, any vortex ring generator can be viewed as a tool for initializing an axisymmetric flow with a particular rate of generation of invariants of motion. Each vortex ring generator has a specific rate for feeding the flow with the kinetic energy, impulse, circulation, *etc.* In this picture, at small strokes (small L/D) one will find that all of the initial vorticity density will coalesce into a steadily translating vortex ring. As the stroke length increases the size and strength of the resulting vortex ring increase. This process persists until a critical formation number is reached, when the vortex generator is not able to provide invariants of motion compatible with a single translating vortex ring. Equivalently, beyond the critical formation number a single vortex ring at equilibrium (steadily translating) that maximizes the mixing entropy for a given energy, impulse and circulation is not possible. In this case the leading vortex ring will pinches off from the trailing jet and will relax to a steadily translating vortex ring with the translational velocity U_{tr} dictated in the maximum entropy principle. For very large strokes (greater than twice the critical formation number) successive vortex rings will pinch-off from the the trailing jet. This scenario was verified in the numerical simulations of the vortex ring pinch-off process.[12] The general observation in these simulations was that the main invariants of motion in the pinch-off process are the kinetic energy, circulation and impulse. The higher enstrophy densities did *not* play a significant role as long as the Reynolds number was relatively high.[13]

It is important to note that the formation number of 4 is only achieved if the rates of generation of the integrals of motion are constant during the formation process. One can change the formation number by varying the rate that the invariants of motion are delivered to the system. This is verified numerically in high Reynolds number flows in Mohseni *et al.*[12] In summary there are two ways to modify the formation number and other properties of the lead-

ing vortex rings:[11,12,14] 1. Time varying speed of the shear layer during the vortex formation 2. Time varying diameter of the shear layer (diameter of the exit). Decelerating the out going fluid slug, which is equivalent to decelerating the exiting shear layer, results in a smaller vortex ring and a smaller formation number. On the contrary accelerating the exiting shear layer during the vortex formation results in a larger vortex ring and a larger formation number.

In the next sections we utilize the same approach to study optimal vortex ring formations at the exit of a shock tube. We view such vortex ring formations as a relaxational process where the generated shear layers relaxes into coherent vortical structures while maximizing a mixing entropy or equivalently extremizing the energy of the system[13] (Kelvin's variational principle).* One also expects that similar optimal vortex ring pinch-off process happens in vortex ring formation at the exit of a shock tube. In fact a close study of the available literature on vortex ring formation at the exit of a shock tube reveals strong indirect evidence for such universality. However, to our knowledge the only systematic experimental investigation on this topic is by Das *et al.*[15] Figure 4 in their article clearly shows a time sequence visualization of such a process. We compare our theoretical predictions with such experimental and numerical studies in section 6.

3 Theory of Shock Tubes

In a shock tube shock waves are usually generated by the sudden rupture of a diaphragm under a compressed gas load. In the analysis of a shock tube presented in this section the gasses will be assumed to be perfect with constant specific heats, and we will ignore viscous effects. While theses assumptions are accurate for low-temperature conditions their fidelity deteriorates at high-temperatures. This analysis, while simple and crude, will be useful for showing the important parameters necessary for the production of strong vortex rings and the conditions for the vortex ring pinch-off at the exit of a shock tube. We assume that at time $t = 0$ the diaphragm separating the low- and high-pressure regions is removed instantaneously. An advantage of vortex ring generation by a shock tube is that the flow field in the tube is well defined and almost perfectly uniform. The velocity history at the exit of a shock tube is ideally a top-hat profile until the leading front of the expansion wave reaches the exit of the shock tube (see figure 2). The potential energy stored in the high pressure gas is utilized in a shock tube to accelerates and later decelerates the fluid almost impulsively, rather than to use the force applied to a piston to do work on the fluid, as with the more conventional vortex-ring generators. Consequently, much higher fluid velocities and accelerations can be achieved.

The shock tube described in figure 1 consists of two sections of low- and high-pressure regions separated by a thin diaphragm. By rupturing this diaphragm a traveling shock wave penetrates the low pressure region, while an expansion wave propagates into the high pressure area. The shock wave travels at a relatively constant Mach number M_s toward the exit of the shock tube, and accelerates the fluid behind it. When the shock wave exit the shock tube an slug of fluid follows the shock and rolls up into a vortex ring. On the other hand the leading front of the expansion waves travels at the speed of sound toward the closed end of the shock tube where they reflect back and proceed toward the exit of the shock tube, while leaving the fluid behind it stationary. The end of the slug of fluid is marked when the expansion waves exit the shock tube and leave the fluid behind them in a relatively stationary state (see Sturtevant[16,17]). There are more complicated interactions in a shock tube that are not considered here. For simplicity we also assume that the shock waves exit the shock tube before the expansion waves reach the exit of the shock tube.

Following a more generally accepted notation, the initial conditions in the low- and high-pressure regions are marked by indices 1 and 4, respectively. As the shock wave propagates into the gas initially at rest (region 1), the state of the gas after the shock wave (region 2) is given by the normal shock wave relationships with $u_1 = 0$ (see, *e.g.*, Liepmann & Roshko[18])

$$\frac{p_2}{p_1} = \frac{M_s^2(1+\alpha_1) - 1}{\alpha_1}; \tag{1}$$

$$\frac{T_2}{T_1} = \frac{p_2}{p_1}\frac{\dfrac{p_2}{p_1} + \alpha_1}{1 + \alpha_1 \dfrac{p_2}{p_1}}; \tag{2}$$

*We would like to point out that similar phenomena is observed in vortex shedding behind bluff bodies where vortices are shed off regularly in an alternating fashion (see Mohseni[14] for details).

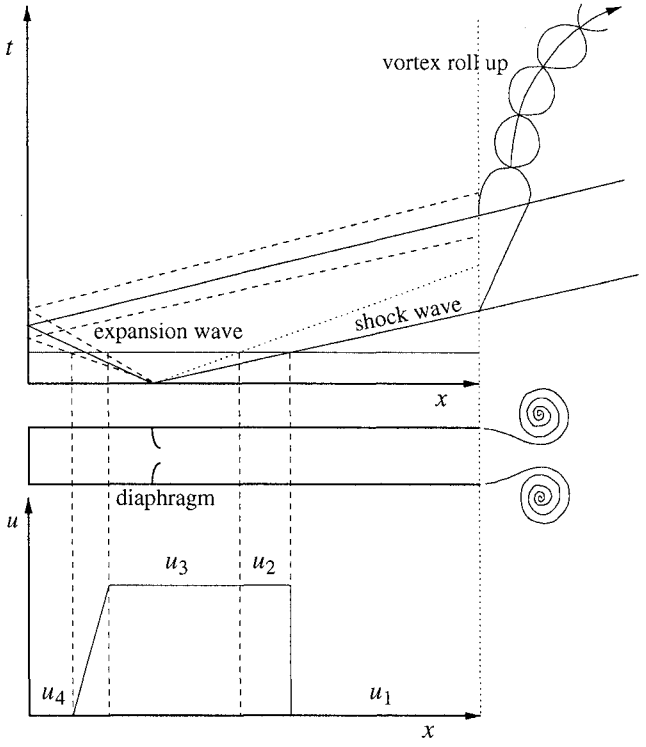

Figure 1: Wave propagations in a shock tube.

$$\frac{u_2}{a_1} = \frac{(\alpha_1 - 1)(\frac{p_2}{p_1} - 1)}{\left((1+\alpha_1)(1+\alpha_1\frac{p_2}{p_1})\right)^{1/2}}; \quad (3)$$

$$\frac{\rho_2}{\rho_1} = \frac{1+\alpha_1\frac{p_2}{p_1}}{\alpha_1+\frac{p_2}{p_1}}; \quad (4)$$

where $\alpha_1 = (\gamma_1+1)/(\gamma_1-1)$. For high temperature conditions produced by the strong shock waves, these equations must be modified to include the real gas effects. The region behind the contact surface is marked as region 3. Regions 2 and 3 are usually separated by an entropy discontinuity at the contact surface which travels with the velocity of the gas in the region 2. The velocities and pressures are the same on both sides of the contact surface

$$u_2 = u_3; \quad (5)$$

$$p_2 = p_3; \quad (6)$$

while the density and temperature could be different.

Simultaneously with the rupture of the diaphragm a centered expansion wave is propagating into the high pressure region (region 4). From the unsteady isentropic expansion, the characteristic quantity $P = \frac{2}{\gamma-1}a+u$ is constant through this expansion fan connecting regions 3 and 4. Therefore, the isentropic relation

$$\frac{p_4}{p_3} = \left(\frac{a_3}{a_4}\right)^{\frac{2\gamma_4}{1-\gamma_4}}; \quad (7)$$

is valid between regions 3 and 4. The expansion wave traveling toward the end wall is of the Q-type while the reflected waves are of the P-type. Now, since the value of P (Riemann invariant) is constant on a P-wave we can write the Riemann invariant

$$u_3 + \frac{2}{\gamma_4-1}a_3 = \frac{2}{\gamma_4-1}a_4; \quad (8)$$

where $u_4 = 0$, and assuming $\gamma_3 = \gamma_4$. One can show that

$$\frac{p_4}{p_1} = \left(1+\frac{2\gamma_1}{\gamma_1+1}(M_s^2-1)\right) \times \left(1+\frac{a_1}{a_4}\frac{\gamma_4-1}{\gamma_1+1}\left(\frac{1}{M_s}-M_s\right)\right)^{\frac{2\gamma_4}{1-\gamma_4}}. \quad (9)$$

This equation relates the shock Mach number to the pressure ratio and sound velocity across the di-

aphragm for a constant-area shock tube. To produce strong shock waves (resulting in stronger vortex rings) a_4/a_1 must be as large as possible. One could show that

$$\left(\frac{a_4}{a_1}\right)^2 = \frac{\gamma_4}{\gamma_1}\frac{m_1}{m_4}\frac{T_4}{T_1} \tag{10}$$

where m is the gas molecular weight. Therefore the sound velocity in the driver section of the shock tube can be increased by using a light gas at high temperature. Another method to increase the shock strength is by using larger tube diameter in the driver section. The shock tube with contraction (variable-area shock tube) can be analyzed similarly and are not presented here.

4 A Model for Vortex Ring Pinch-off Process at the Exit of a Shock Tube

Our objective in this section is to calculate the length of the fired slug of fluids from a shock tube based on the initial states of the gases in the driver and driven sections of the shock tube. It is believed that there is a similarity between the vortex ring generation at the exit of a shock tube and the vortex ring formation in a cylinder piston mechanism.[11] In both cases an impulsive movement of a slug of fluid generates a cylindrical shear layer that roles up into a vortex ring. The length of the ejected slug of fluid determines the size of the resulting vortex ring. Therefore, to generate energetic thin-cored vortex rings it is important that a relatively short slug of fluid be ejected at high velocity. We will derive equations for the equivalent slug of fluid for any initial conditions in the low- and high-pressure sections of a shock tube.

Consider the simple shock tube in Fig. 1. The low- and high-pressure sections are initially separated by a diaphragm. The tube diameter is D, length of the driver section (high-pressure region) is l_h, and the length of the low pressure section (low-pressure region) is l_l. The rupture of the diaphragm generates a shock wave that travels into the low pressure section. Immediately after the rupture of the diaphragm the high pressure gas is expanded into the low pressure section of the shock tube. This generates an expansion wave that travels into the high pressure section of the shock tube from the initial position of the diaphragm at the local speed of sound.

The operation of a shock tube can be easily explained in the $x-t$ diagram in Fig. 1. Regions (1) and (4) are the initial states of the low- and high-pressure sections of the shock tube, respectively. A relatively steady flow of fluids at velocity u_2 will follow the exiting shock and will persist until the reflected expansion waves from the end wall reaches the exit of the shock tube and signal the flow that the fluid behind them is stationary. Therefore, the total duration for the exiting slug of fluid at velocity u_2 is the time between the exit of the shock wave and the exit of the expansion waves (see figure 2). This qualitative description was suggested by Sturtevant.[16,17] Here we quantitatively calculate it based on the initial conditions of regions 1 and 4. The expansion waves have a leading front and a tailing front. nonsimple effects due to the interaction of the expansion waves with the end wall.

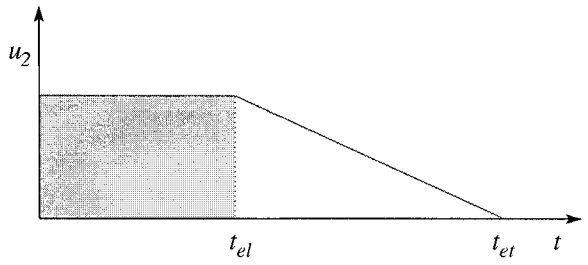

Figure 2: Typical exit velocity profile for shock tubes with relatively long driver section.

After the rupture of the diaphragm the nondimensional time† for the shock wave to reach the exit is

$$t_s^* := \frac{u_2 t_s}{D} = \frac{u_2}{D}\frac{l_l}{a_1 M_s} = \frac{l_l^*}{\frac{a_1 M_s}{u_2}}. \tag{11}$$

Substituting M_s from equation (1) and u_2/a_1 from equation (3) one can write

$$t_s^* := \frac{l_l^*(\alpha_1 - 1)(p_{21} - 1)}{1 + \alpha_1 p_{21}}. \tag{12}$$

Similar quantity for the tailing front of the expansion wave to reach the exit of the shock tube is approxi-

†Nondimensionalized by the diameter D and the exit velocity u_2. The intrinsic scalings in this case are the translational velocity U_{tr} and the diameter D_r of the leading vortex ring. However D_r/D and U_{tr}/u_2 are usually constant after the vortex formation. Therefore, one can equivalently use the more accessible quantities D and u_2 for nondimensionalization.

mately

$$t^*_{et} := \frac{u_2 t_{et}}{D} = \frac{u_2}{D}\left(\frac{l_h}{a_3 - u_3} + \frac{l_h + l_l}{a_4}\right) = \frac{l^*_h}{\frac{a_3 - u_3}{u_2}} + \frac{l^*_h + l^*_l}{\frac{a_4}{u_2}}; \qquad (13)$$

where $l^* = l^*_h + l^*_l$. The leading front of the expansion wave travels into the high-pressure region at the sound speed a_4. The reflected rarefaction wave at the end wall proceeds toward the shock tube exit with the speed of $a_3 + u_3$. The propagation speed of this wave will change to $a_2 + u_2$ (note that $u_2 = u_3$) if the leading front of the expansion wave catches up with the contact surface before it reaches the exit of the tube. Therefore, one needs to check if the leading front of the expansion wave catches up with the contact surface moving at the speed $u_2 = u_3$ inside the low-pressure section of the shock tube. At such an instance, $t_{inc} = X/u_2$, both the contact surface and the leading front of the expansion waves will be at location X. The origin of the coordinate system is placed at the initial location of the diaphragm. X is calculated by equating the elapsed time to reach this location for both the contact surface and the leading front of the expansion wave

$$t_{inc} = \frac{X}{u_2} = \frac{l_h}{a_4} + \frac{l_h + X}{a_3 + u_3}.$$

Hence

$$X^* := \frac{X}{D} = \left(1 + \frac{u_2}{a_3}\right)\left(\frac{l^*_h}{\frac{a_4}{u_2}} + \frac{l^*_h}{\frac{a_3}{u_2} + 1}\right)$$

Therefore, the nondimensional time for the leading front of the expansion wave to reach the exit of the tube is

$$t^*_{el} := \frac{u_2 t_{el}}{D} = \frac{u_2}{D}\left(\frac{l_h}{a_4} + \frac{l_h + l_l}{a_3 + u_3}\right) = \frac{l^*_h}{\frac{a_4}{u_2}} + \frac{l^*_h + l^*_l}{\frac{a_3 + u_3}{u_2}}, \quad \text{if} \quad X > l_l; \qquad (14)$$

$$t^*_{el} := \frac{u_2 t_{el}}{D} = \frac{X}{D} + \frac{u_2}{D}\left(\frac{l_l - X}{a_2 + u_2}\right) = X^* + \frac{l^*_l - X^*}{\frac{a_2}{u_2} + 1}, \quad \text{if} \quad X \le l_l. \qquad (15)$$

The approximated elapsed time t_e for the expansion waves to reach the exit of the shock tube will characterize the total duration of the slug by $t_e - t_s$. The nondimensional length of the resulting slug of fluid is then given by

$$L^* := \frac{L}{D} = \frac{u_2(t_e - t_s)}{D} = t^*_e - t^*_s. \qquad (16)$$

This relation gives the length of the exiting slug of fluid as a function of the initial conditions in the low- and high-pressure regions. By knowing T_1, T_4, p_1, p_4, the fluid parameters, and the geometrical characteristics of the driver and driven sections of the shock tube one can calculate the duration (an consequently the length of the slug) for the exiting fluid the shock tube.

5 Computational Procedure

Our objective in this section is to calculate the initial condition for the vortex ring pinch-off at the exit of a shock tube. Practically we look for the limiting conditions that separate the pinched off cases from the non pinched ones. In doing so we seek the initial conditions that result in the total length of the exiting slug of fluid to be 4 times the exit diameter as predicted by the model in Mohseni *et al.*[10–12] Given the initial conditions in the low- and high-pressure regions, equation (9) can be used to calculate the shock Mach number M_s. This equation needs to be solved iteratively. Knowing M_s, p_2/p_1 can now be calculated using equation (1).

We need to calculate a_3/u_2 from the initial states. Using equations (8) and (7), one can write

$$\frac{a_3}{u_2} = \frac{\gamma_4 - 1}{2}\frac{1}{\frac{a_3}{a_4} - 1}.$$

However, using equation (8), $u_2 = u_3$, and $p_2 = p_3$ one can write

$$\frac{a_3}{u_2} = \frac{\gamma_4 - 1}{2}\frac{1}{\left(\frac{p_4}{p_1}\frac{p_1}{p_2}\right)^{\frac{\gamma_4 - 1}{2\gamma_4}} - 1};$$

where p_4/p_1 is given by equation (9) and p_1/p_2 is given by equation (1). Now that a_3/u_2 is calculated one can easily compute a_4/u_2 from equation (8) as

$$\frac{a_4}{u_2} = \frac{a_3}{u_2} + \frac{\gamma_4 - 1}{2}.$$

a_2/u_2 is required in calculating X, and can be calculated by noting that

$$\frac{a_2}{u_2} = \frac{a_2}{a_1}\frac{a_1}{u_2};$$

and using equation (3) and

$$\left(\frac{a_1}{a_2}\right)^2 = \frac{T_1}{T_2} = \frac{p_2}{p_1}\frac{\dfrac{p_2}{p_1}+\alpha_1}{1+\alpha_1\dfrac{p_2}{p_1}}.$$

At this point all the terms on the right hand side of equation (16) are described in terms of known quantities. Therefore, the stroke ratio of the equivalent slug model in the shock tube mechanism is given by equation (16) in terms of the known initial conditions in the low- and high-pressure regions of the shock tube.

Mohseni & Gharib[11] offered a model for the vortex ring pinch-off process by equating the invariants of motion of the system initially and after the vortex ring formation. The initial state was approximated by a fluid slug moving at a fixed velocity and the final state was approximated by a vortex in the Norbury family of vortices.[20] They predicted an average formation number around 4. The same technique can be used in the case considered in this study. We calculated the length of the slug of fluid in a compressible process. Therefore, by substituting the formation number by 4 in equation (16) we obtain a relation to calculate the pressure ratio p_4/p_1 for any given temperature ratio T_4/T_1. It is clear that such a relation depends on how the arrival of the end of the slug of fluid is marked in defining t_e^* in equation (16). The optimal vortex ring with maximal circulation will be generated for the formation number of 4 and by marking the end of the slug of fluid by the emergence of the leading front of the expansion wave from the shock tube $t_e^* = t_{el}^*$.

6 Comparison with Experimental and Computational Data

In this section the pinch-off criteria predicted in the previous sections will be contrasted with available experimental and numerical data. All of the cases considered here are summarized in Table 1.

Recently Das *et al.*[15] carried out experiments on the vortex ring formation at the exit of a shock tube where they observed vortex ring pinch-off process. Knowing the length of the slug of fluid emerging from the shock tube, for any given initial conditions, one can use the vortex ring pinch-off criteria proposed by Mohseni & Gharib[11] to predict the pinch-off at the exit of a shock tube. This is done in figure 3 for the initial conditions of case A1 in Table 1. Similar results for the cases considered in Elder & de Haas[21] are presented in figure 4.

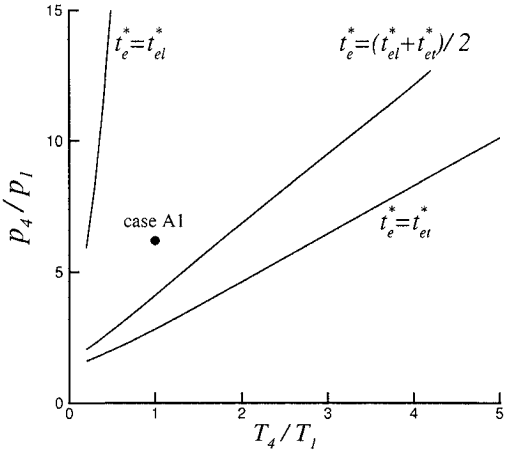

Figure 3: Vortex ring pinch-off criteria for experimental setup in case A1 in Table 1 from Das *et al.*[15] $l_h^* = 12.7/5.2 = 2.44$ and $l_l^* = 105/5.2 = 20.19$.

The lines marked by $t_e^* = t_{el}^*$ in figures 3 and 4 are calculated from equation (16) by marking the end of the fluid slug by the initial emergence of the leading front of the expansion wave from the shock tube. In the region above this line one is guaranteed to have a vortex ring pinch-off with the formation number 4, uniform fluid slug velocity of u_2 during the pinch-off, and with the nondimensional energy, E_{nd}, and circulation Γ_{nd}, of the leading vortex ring as predicted in Mohseni & Gharib.[11] That is $E_{nd} = E/(\Gamma^{3/2}I^{1/2}) \approx 0.3$ and $\Gamma_{nd} = \Gamma/(I^{1/3}U_{tr}^{2/3}) \approx 2$. Note that all the quantities in these relations need to be calculated in the frame of reference of invariants of motion that is moving with the speed of the leading vortex ring. For all the initial conditions below the line marked by $t_e^* = t_{el}^*$ we expect that $E_{nd} > 0.3$ and $\Gamma_{nd} < 2$.

The lines marked by $t_e^* = t_{et}^*$ are calculated from equation (16) by marking the end of the fluid slug by the time that the tailing front of the expansion waves arrives at the shock tube exit. The region below this line characterizes the vortex ring formation without a pinch-off process; We predict no trailing jets following the leading vortex ring in this region. In the region between the line $t_e^* = t_{el}^*$ and $t_e^* = t_{et}^*$ there is a possibility of vortex ring pinch-off at a smaller formation number.

Note that in the region below the lines marked by $t_e^* = t_{el}^*$ there is a deceleration in the exit velocity of the slug of fluid due to the expansion fan.

Case	l_l	l_h	D	D_n	$\frac{p_4}{p_1}$	$\frac{T_4}{T_1}$	Reference
A1	105 cm	12.7 cm	5.2 cm	5.2 cm	6.2	1	Das *et al.*[15]
A2	105 cm	5.1 cm	5.2 cm	5.2 cm	4.1	1	Das *et al.*[15]
B1	176 in	24 in	3.375 in	3.375 in	3.72	1	Elder & de Haas[21]
B2	176 in	24 in	3.375 in	3.375 in	1.68	1	Elder & de Haas[21]
C1	1250 mm	100 mm	40 mm	6 mm	5	1	Minota *et al.*[22]
D1	160 cm	15 cm	7.2 cm	7.2 cm	2.36	1	Sturtevant[16]
D2	160 cm	10 cm	7.2 cm	7.2 cm	2.36	1	Sturtevant[16]
D3	160 cm	5 cm	7.2 cm	7.2 cm	2.36	1	Sturtevant[16]
D4	160 cm	2.5 cm	7.2 cm	7.2 cm	2.36	1	Sturtevant[16]

Table 1: Parameters for experimental cases considered in this study.

This is equivalent to decelerating an exiting shear layer suggested in Mohseni & Gharib[11] and studied numerically in Mohseni *et al.*[12] As suggested and verified in those studies one expects the observed formation number for a pinched off vortex ring to be smaller that 4. This decrease in the formation number was observed by Das *et al.*,[15] and it is only a consequence of the geometrical characteristics of their shock tube and the chosen initial conditions. In their case the length of driver section is relatively short and the length of the driven section is relatively long. Consequently, the leading front of the expansion wave will quickly reflects back from the wall at the end of the driver section and follows the shock wave. Usually the leading expansion wave travels at a lager velocity of $a_3 + u_2$ than the shock wave velocity. Therefore, the longer the length of the driven section the shorter the length of the uniform slug of fluid with velocity u_2. In fact for shock tubes with a very long driven section the leading front of the expansion wave might even catch up with the shock wave. As it is clear from figure 3 the cases considered by Das *et al.*[15] do not have a uniform exit velocity u_2 during the entire vortex ring formation process. The last stage of the formation process in the cases considered by them is significantly affected by the exit of the expansion wave and its consequent deceleration in the exit velocity u_2. We predict that in their cases $E_{nd} > 0.3$ and $\Gamma_{nd} < 2$. To guarantee the formation of optimal vortex rings with formation number 4 one requires to be above the line marked by $t_e^* = t_{el}^*$, where the exit velocity during the vortex formation is uniformly u_2. In fact one can generate an even stronger vortex ring if the exit velocity is accelerated at the final stage of the vortex ring formation.[12]

Elder & de Haas[21] used a relatively long high pressure chamber. See cases B1 and B2 in Table 1. Consequently, they had a better chance for generating optimal vortex rings at lower pressure ratios p_4/p_1. This is clear in figure 4 where the pinch-off curves have smaller slopes than the corresponding curves in figure 3 generated for the data from Das *et al.*[15] The photographs of the vortex rings generated in experiments by Elder & de Haas,[21] however, were reported only for the initial phase of the vortex propagation where the vortices were very close to the exit of the shock tube or just focusing on the leading vortex ring and not its possible trailing jets. As a result, Elder & de Haas[21] did not provide enough experimental information to verify the pinch-off process in their experiments.

Case C in Table 1 represents a case where the inner diameter of the shock tube is significantly different than the diameter of the the exit nozzle. Such a change could result in a new formation number defined based on the nozzle diameter and with longer fluid slug with uniform velocity. This case was investigated by Minota *et al.*[22] in a study of shock formation by compressible vortex rings impinging on a wall. There are evidence of a vortex ring pinch-off process in figures 4 and 6 of Minota *et al.*[22] They placed a glass wall at a distance of 2.7 times the nozzle diameter away from the nozzle. Therefore, The exiting shock wave from the shock tube will quickly reflects back from the glass wall and interacts with the exiting shear layer from the shock tube. This makes it difficult to make a conclusion about the pinch-off process in their experiments and computations.

Sturtevant[16] (cases D in Table 1) clearly noticed the significance of the length of the pressurized chamber in defining the length of the fluid slug exiting from the shock tube. However, Sturtevant used

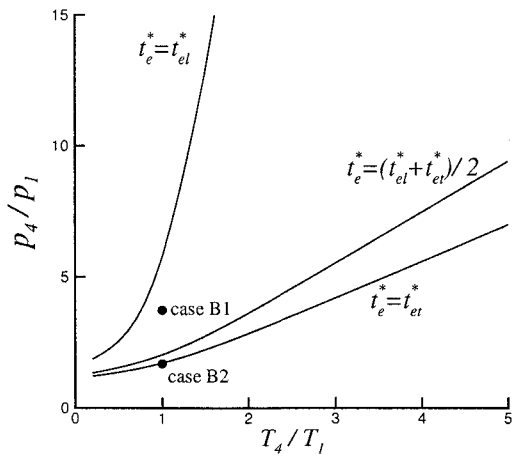

Figure 4: Vortex ring pinch-off criteria for experimental setup in cases B1 and B2 in Table 1 from Elder & Haas.[21] $l_h^* = 24/3.375 = 7.11$ and $l_l^* = 176/3.375 = 52.15$.

Helium in the pressurized chamber. Helium has a lower molecular weight, $m_4 = 4$, than the air in the low pressure region, $m_1 = 28.97$. Consequently, the speed of sound in the high-pressure section was much higher, resulting in shorter time for the expansion waves to reach the exit of the tube. This will be evident from the speed of sound

$$a_4 = \sqrt{\gamma_4 \frac{\overline{R}}{m_4} T_4},$$

where $\overline{R}$ is the universal gas constant. Therefore the length of the resulting fluid slugs in Sturtevant's experiments are relatively small; They have small formation numbers and his test cases resides below the critical $(p_4/p_1) - (T_4/T_1)$ curve for a pinch-off. The significant difference between the molecular weight of air and helium would also brings more complications due to mixing of a heavy and light gases.

7 Conclusions

The optimal formation of vortex rings at the exit of a shock tube was studied theoretically. A model for predicting the maximum circulation that a vortex ring can attain at the exit of a shock tube was offered. The formation of vortex rings at high Reynolds numbers is mainly an inviscid problem governed by the integrals of motion. It is predicted that if the rate of generation of the integrals of motion at the exit of the shock tube is constant during the vortex ring formation (the shaded region in figure 2), and if the shear layer is sufficiently thin (and the Reynolds number sufficiently high) the leading vortex ring pinches off with normalized energy E_{nd} and circulation Γ_{nd} of about 0.3 and 2.0, respectively. The main invariants of motion are the energy E, impulse I, circulation Γ, and the translational velocity U_{tr}. These invariants of motion define an intrinsic scaling for vortex ring formations. An observer in the intrinsic frame of reference is attached to the vorticity center of the leading vortex ring and is moving with the translational velocity U_{tr} of the leading vortex ring. Since the ratios U_{tr}/u_2 and D_{ring}/D_n (D_n is the nozzle diameter and u_2 is the fluid velocity behind the shock wave) are usually constant it is easier to nondimensionalize based on u_2 and D_n.

To achieve maximum circulation the initial conditions and the design of the driver and driven sections must be such that the generated shock wave reaches the shock tube exit at least $4D_n/u_2$ time units before the leading front of the expansion waves arrives at the shock tube exit. A simple way to satisfy this condition is to design a shock tube with long driver and short driven sections. At high Reynolds number and with thin shear layers, the rate of generation of the integrals of motion needs to be modified as a function of time in order to change the formation number of the leading vortex ring. This statement is based on the observation that the leading vortex ring will pinch off when the generating mechanism is not capable of providing energy and circulation at a rate compatible with the normalized circulation and energy corresponding to a steadily translating vortex ring. A dynamic interpretation of the pinch off process suggests that the deceleration of the slug of fluid due to the arrival of the expansion waves at the shock tube exit results in an early pinch off and smaller formation number. However, in a shock tube the maximum circulation of the leading vortex ring is achieved when the length of the exiting and uniform slug of fluid (before the emergence of the leading front of the expansion wave from the shock tube) is at least four times the exit diameter. Finally, the model is verified by comparison with the available computational and experimental data.

Acknowledgments

The author would like to acknowledge his conversations with Professor B. Sturtevant in 1999 when the

author, motivated by figures 5b and 6b in Minota *et al.*,[22] attempted to model vortex ring pinch-off process at the exit of a shock tube. Professor Sturtevant generously provided copies of his AFOSR annual contract reports.[16,17] Sturtevant's ideas in those reports were instrumental in the development of the model developed in this study.

References

[1] P. Vieille. Sur les discontinuities produites par la detente brusque de gaz comprimes. *Comptes Rendus de l'Academie des Sciences*, 129:1228–1230, 1899.

[2] T. von Karman and J.M. Burgers. *Aerodynamic Theory*, volume II. 1935.

[3] Gawthrop, Shepherd, and Perrott. *J. Franklin Inst.*, 211:67–86, 1931.

[4] B. Sturtevant. Shock waves in non-uniform media: real-life gas dynamics. In *Shock Tube and Shock Wave Research*, page 12, University of Washington, Seattle, 1977. Birkhuser Boston, Boston, MA.

[5] D.W. Moore and D.I. Pullin. On steady compressible flows with compact vorticity; the compressible Hill's spherical vortex. *J. Fluid Mech*, 374(1):285–303, 1998.

[6] D.I. Pullin. Vortex ring formation in tube and orifice openings. *Phys. Fluids*, 22:401–403, 1979.

[7] N. Didden. On vortex formation and iteraction with solid boundaries. In H.G. Hornung and E.A. Muller, editors, *Vortex Motion*, page 1. Braunschweig: Vieweg, 1982.

[8] K. Mohseni. Mixing and impulse extremization in microscale vortex formation. In *to be published in the Proceedings of the Fifth International Conference on Modeling and Simulation of Microsystems*, San Juan, Puerto Rico, April 2002.

[9] K. Shariff and A. Leonard. Vortex rings. *Ann. Rev. Fluid Mech.*, 34:235–279, 1992.

[10] M. Gharib, E. Rambod, and K. Shariff. A universal time scale for vortex ring formation. *J. Fluid Mech*, 360:121–140, 1998.

[11] K. Mohseni and M. Gharib. A model for universal time scale of vortex ring formation. *Phys. Fluids*, 10(10):2436–2438, 1998.

[12] K. Mohseni, H. Ran, and T. Colonius. Numerical experiments on vortex ring formation. *J. Fluid Mech*, 430:267–282, 2001.

[13] K. Mohseni. Statistical equilibrium theory of axisymmetric flows: Kelvin's variational principle and an explanation for the vortex ring pinch-off process. *Phys. Fluids*, 13(7):1924–1931, 2001.

[14] K. Mohseni. Studies of two-dimensional vortex streets. AIAA paper 2001-2842, June 2001. 31st AIAA Fluid Dynamics Conference and Exhibit, Anaheim, CA.

[15] D. Das, J.H. Arakeri, A. Krothapalli, and L. Lourenco. Compressible vortex ring: A PIV study. AIAA paper 2001-2214, May 2001. 7^{th} AIAA/CEAS Aeroacoustics Conference, Maastrich, Netherlands.

[16] B. Sturtevant. Dynamics of vortices and shock waves in nonuniform media. AFOSR-TR 79-0898, Air Force Office of Scientific Research, 30 June 1979.

[17] B. Sturtevant. Dynamics of turbulent vortex rings. AFOSR-TR 81-0400, Air Force Office of Scientific Research, 31 January 1981.

[18] H.W. Liepmann and A. Roshko. *Elements of Gasdynamics*. Wiley, New York, 1957.

[19] J.D. Anderson. *Modern Compressible Flow*. McGraw Hill, Inc, 1990.

[20] J. Norbury. A family of steady vortex rings. *J. Fluid Mech*, 57(3):417–431, 1973.

[21] F.K. Elder and N. de Haas. Experimental study of the formation of a vortex ring at the open end of a cylindrical shock tube. *J. Appl. Phys.*, 23(10):1065–1069, 1952.

[22] T. Minota, M. Nishida, and M.G. Lee. Shock formation by compressible vortex ring impinging on a wall. *Fluid Dynamics Research*, 21:139–157, 1997.